Original papers
Materials for energy and environment, next-generation photovoltaics, and green technologies

УДК 661.965+544.723.2 DOI: 10.17277/jamt-2025-10-04-342-350

Hydrogen separation from gas mixtures: evaluation of adsorbent performance using the IAST model

© Nikita S. Krysanov[a], Elena A. Berdonosova[a], Semen N. Klyamkin[a]✉

[a] *Lomonosov Moscow State University, 1/3, Leninskie Gory, Moscow, 119991, Russian Federation*

✉ klyamkin@highp.chem.msu.ru

Abstract: Samples of commercial adsorbents – activated carbon (AC), zeolite (ZS), and silica gel (SG) – were studied in the adsorption processes of hydrogen, methane, nitrogen, carbon dioxide, and carbon monoxide in order to assess their efficiency for hydrogen purification from gas impurities. The composition and morphology of the materials were characterized using scanning electron microscopy and energy-dispersive X-ray microanalysis. Textural properties (specific surface area and pore structure) were determined from nitrogen cryosorption data using the BET, Gurvich, and BJH models. Adsorption isotherms were obtained for all studied gases at pressures up to 25 atm and temperatures ranging from 0 to 50 °C. Isosteric heats of adsorption and ideal selectivities for the "impurity gas – hydrogen" pairs were calculated. To evaluate the behavior of the studied adsorbents toward multicomponent gas mixtures, simulations were performed using the Ideal Adsorbed Solution Theory (IAST). This approach revealed that in real mixtures, the selectivity $S_{IAST}(CO_2/H_2)$ increases by a factor of 1.5–3 compared to the values estimated from single-gas data.

Keywords: hydrogen; pressure swing adsorption; adsorbents; Ideal Adsorbed Solution Theory (IAST).

For citation: Krysanov NS, Berdonosova EA, Klyamkin SN. Hydrogen separation from gas mixtures: evaluation of adsorbent performance using the IAST model. *Journal of Advanced Materials and Technologies*. 2025;10(4):342-350. DOI: 10.17277/jamt-2025-10-04-342-350

Выделение водорода из газовых смесей: оценка эффективности адсорбентов с применением модели IAST

© Н. С. Крысанов[a], Е. А. Бердоносова[a], С. Н. Клямкин[a]✉

[a] *Московский государственный университет имени М. В. Ломоносова, Ленинские горы, 1/3, Москва, 119991, Российская Федерация*

✉ klyamkin@highp.chem.msu.ru

Аннотация: Образцы коммерческих адсорбентов активированного угля AC, цеолита ZS и силикагеля SG были исследованы в процессах адсорбции водорода, метана, азота, углекислого и угарного газа для оценки эффективности их использования при очистке водорода от газовых примесей. Методами сканирующей электронной микроскопии и энергодисперсионного микроанализа охарактеризованы состав и морфология материалов. Текстурные характеристики (удельная поверхность и характер пористости) рассчитаны по моделям БЭТ, Гурвича и BJH на основе данных по криосорбции азота. Для всех изученных газов построены изотермы адсорбции в области давлений до 25 атм при температурах от 0 до 50 °C, определены изостерические теплоты адсорбции, рассчитаны идеальные селективности в парах «примесный газ – водород». Для оценки поведения изученных адсорбентов по отношению к многокомпонентным газовым смесям проведено моделирования с использованием теории идеальных адсорбированных растворов (IAST). Данный подход позволил установить, что в реальных смесях селективность $S_{IAST}(CO_2/H_2)$ увеличивается в 1,5–3 раза по сравнению с расчетами по данным для индивидуальных газов.

Ключевые слова: водород; короткоцикловая адсорбция; адсорбенты; теория идеальных адсорбированных растворов (IAST).

Для цитирования: Krysanov NS, Berdonosova EA, Klyamkin SN. Hydrogen separation from gas mixtures: evaluation of adsorbent performance using the IAST model. *Journal of Advanced Materials and Technologies*. 2025;10(4):342-350. DOI: 10.17277/jamt-2025-10-04-342-350

1. Introduction

At present, the main method for producing hydrogen is its extraction from the products of natural gas steam reforming or purification of by-product gases from oil refineries [1, 2]. Three primary methods are currently used for separating hydrogen-containing gas mixtures: partial condensation, pressure swing adsorption (PSA), and membrane gas separation [3].

Hydrogen purification is most commonly carried out by pressure swing adsorption (PSA)**,** which is based on the preferential adsorption of impurities when a gas mixture is passed under high pressure through an adsorbent bed, followed by desorption upon pressure reduction [4, 5]. Activated carbons, zeolites, and silica gels are typically used as adsorbents in PSA systems [6, 7].

Activated carbon is a highly porous carbon material obtained from various precursors such as coal, petroleum, or plant-based sources. Different activation methods yield carbons with a wide range of pore volumes, structures, and surface chemical compositions. The average pore size varies from 35 Å to 2050 Å. For example, BPL-grade activated carbon has a surface area of 1100 $m^2 \cdot g^{-1}$ and a pore volume of 0.7 $cm^3 \cdot g^{-1}$, making it suitable for hydrogen purification by PSA [8].

Zeolites are aluminosilicates with a three-dimensional framework of $[XO_4]$ tetrahedra, where X = Al or Si. They are classified according to their Si/Al ratio: type A zeolites (Si/Al ~ 1.0), type X (Si/Al ~ 1.0–1.5), and type Y (Si/Al ~ 1.5–3.0). In industry, calcium-exchanged zeolite 5A – with a pore size of 5 Å and a surface area of 460–480 $m^2 \cdot g^{-1}$ is commonly used for hydrogen purification [9–11].

Silica gel is a porous amorphous form of silicon dioxide with an interconnected pore network. Depending on the synthesis method, it can have micropores (S_{sp} ~ 700–800 $m^2 \cdot g^{-1}$), mesopores (S_{sp} ~ 520 $m^2 \cdot g^{-1}$), or macropores (S_{sp} ~ 320 $m^2 \cdot g^{-1}$). The Sorbead® H grade of silica gel, containing 3–4 % aluminum oxide, has a surface area of 750 $m^2 \cdot g^{-1}$ and a pore volume of 0.5 $cm^3 \cdot g^{-1}$, making it an effective adsorbent for hydrogen purification [12, 13].

The evaluation of hydrogen purification efficiency on each adsorbent was performed using simulations based on the Ideal Adsorbed Solution Theory (IAST). The IAST assumes that adsorbed molecules form an ideal solution on the adsorbent surface. In this model, the adsorbent is considered thermodynamically inert with a constant surface area, and adsorption is described through the Gibbs approach [14]. It has been shown that IAST-based modeling provides results more rapidly than grand canonical Monte Carlo simulations [15]. For the calculations, a specialized Python-based program under the MIT license (pyIAST) was used [16].

The aim of this work is to characterize the adsorbents AC, SG, and ZS, and to evaluate their performance in hydrogen separation from gas mixtures using the IAST model.

2. Materials and Methods

2.1. Initial materials

For characterization, specific samples of commercial adsorbents provided by the scientific and industrial company Grasys (Moscow) were selected for testing: activated carbon AC, silica gel SG, and zeolite ZS. These materials are considered potential alternatives to the adsorbents currently used in industrial PSA units.

2.2. Research methods

The morphology of the materials was examined using a TESCAN Vega3 XM scanning electron microscope (SEM) at an accelerating voltage of 10 kV. Both secondary and backscattered electron detectors were employed, and the sample surfaces were gold-coated to ensure electrical conductivity. Elemental composition was determined using an Oxford Instruments INCA X-act energy-dispersive (EDX) microanalyzer.

X-ray diffraction (XRD) data were collected at room temperature using a Thermo ARL X'TRA powder diffractometer with CuKα radiation (λ = 1.5405 Å). Measurements were performed in reflection geometry using a semiconductor Peltier detector, over a 2θ range of 5° to 65° with a scanning rate of 0.5°·min^{-1}.

The porous structure of the samples was investigated by nitrogen cryosorption at –196 °C using an IMC Prosurf-v1220 instrument. Prior to measurements, the samples were degassed under vacuum ($5.0 \cdot 10^{-3}$ mmHg) and activated at different temperatures: 200 °C for activated carbon, 130 °C for silica gel, and 150 °C for zeolite. The specific surface area was calculated using the BET model in the relative pressure range of (0.05–0.35)p/p_0, while the total pore volume was determined by the Gurvich method at 0.97 p/p_0. The pore size distribution was derived using the BJH method.

Excess gas adsorption on the sorbent surface was measured by the volumetric (Sieverts) method. Adsorbent granules (3–5 g) were placed in an

autoclave, which was degassed to $5.0 \cdot 10^{-3}$ mmHg and activated at specific temperatures. After cooling, the autoclave was placed in a thermostat to achieve thermal equilibrium. Temperature control was maintained using an ice bath and a high-precision water thermostat, with temperature stability of ±0.2, ±0.3, and ±0.1 °C depending on the experiment.

The autoclave volume was calibrated using helium. For measurements conducted at non-room temperatures, the volumes of the apparatus parts held at different temperatures were accounted for. The amount of adsorbed gas was determined from manometric measurements by calculating the difference between the introduced gas mass m_0 and the residual mass m_1. The difference between the masses m_0 and m_1 yielded the mass of the adsorbed gas Δm. Gas densities were obtained from the Thermophysical Properties of Fluid Systems database [17].

Uncertainties in pressure and temperature measurements resulted in adsorption errors of ±0.032 mmol·g^{-1} for CO_2, CO, CH_4 и N_2 and ±0.017 mmol·g^{-1} for H_2 at 25 atm.

To describe the excess adsorption isotherms, high-degree polynomial fits were applied using OriginPro software, with a coefficient of determination $R^2 > 0.9998$**.** The isosteric heat of adsorption for CH_4, CO_2, N_2, CO и H_2 was determined from the slope of the isosteres, which relate the logarithm of equilibrium gas pressure to the reciprocal of temperature at constant adsorption. The uncertainty in the isosteric heat Q_{isost} was estimated using the least squares method**.** Measurements were conducted for the adsorption of each of the five gases at three temperatures: 0, 22, and 50 °C.

3. Results and Discussion

To determine the chemical composition and surface morphology, the adsorbent samples were analyzed using energy-dispersive X-ray spectroscopy and SEM.

The high oxygen content in the activated carbon AC (8 wt. %) indicates the presence of oxygen-containing functional groups. The silica gel SG showed a lower oxygen content (42 wt. %) and an elevated carbon content (11 wt. %), which may be attributed to surface contamination during synthesis. The chemical composition of the zeolite ZS corresponds to that of calcium zeolite A (Si:Al ~ 1.0).

Figure 1 presents SEM-images of the adsorbent particle surfaces at both low and high magnifications.

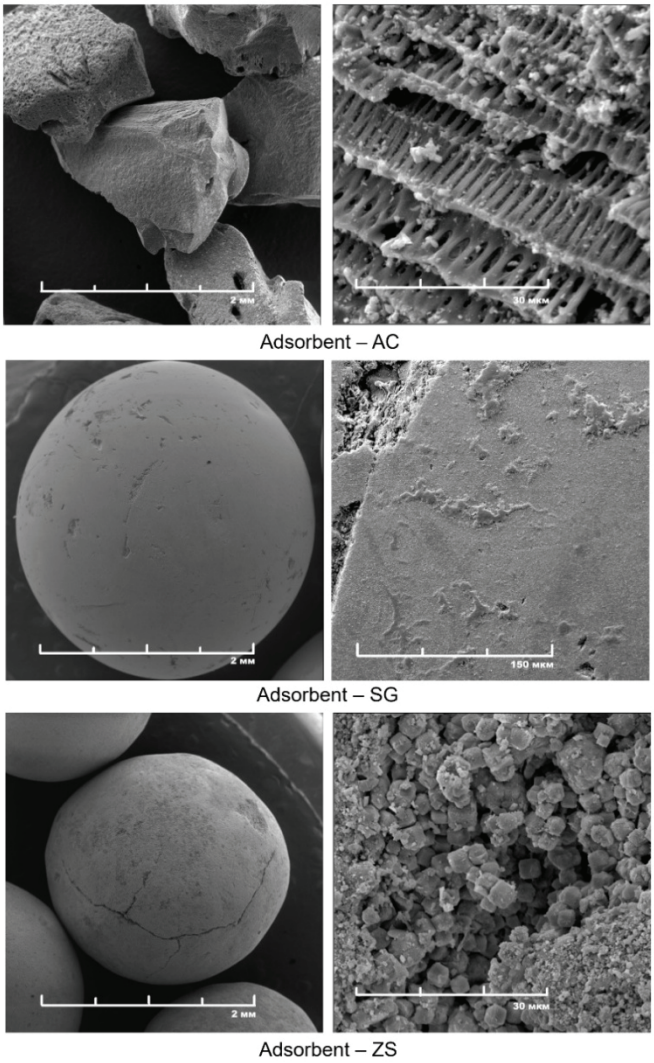

Fig. 1. SEM-images of the adsorbent surfaces

The activated carbon granules have sizes of approximately 1.5–2.0 mm, featuring an irregular surface and layered structure. In contrast, the silica gel SG and zeolite ZS granules exhibit a rounded shape with diameters of about 2.5–3.0 mm; their surfaces also display defects, chips, and cracks.

The classification of the adsorbents as crystalline or amorphous materials was performed using X-ray diffraction (XRD) analysis.

The XRD pattern of the activated carbon shows two broad peaks at 23° and 43°, corresponding to the (002) and (100) reflections of graphite. The average widths of these peaks were used to calculate the crystallite dimensions along the basal plane L_a and perpendicular to it L_c using the Scherrer equation [18].

The obtained values, $L_a = 3.51$ nm and $L_c = 1.02$ nm, indicate the presence of nanosized graphite crystallites within the activated carbon.

Table 1. Adsorption characteristics of the studied sorbents

Adsorbent	Activated carbon AC	Silica Gel SG	Zeolite ZS
S_{sp}, $m^2 \cdot g^{-1}$	994	741	408
V_{pore}, $cm^3 \cdot g^{-1}$	0.44	0.40	0.25
Fraction, %:			
micropore	92	79	88
mesopore	7	20	9
macropore	1	1	3

The XRD pattern of the zeolite ZS exhibits a series of narrow, intense peaks, confirming its crystalline nature. Analysis of the diffraction data showed that zeolite ZS crystallizes in a cubic unit cell (space group $Fm\bar{3}m$) with a lattice parameter of $a = (2.34 \pm 0.02)$ Å, consistent with calcium zeolite 5A ($Fm\bar{3}m$, $a = 12.32$ Å) [19].

The specific surface area (S_{sp}, $m^2 \cdot g^{-1}$) of the adsorbents was measured by nitrogen cryosorption and processed using the BET theory. The total pore volume (V_{pore}, $cm^3 \cdot g^{-1}$) and pore size distribution were determined from the BET isotherms using the Gurvich and BJH methods, respectively. The adsorption characteristics calculated from the isotherm data are presented in Table 1.

The obtained values of specific surface area and pore volume are consistent with literature data for similar adsorbents [20]. The activated carbon AC exhibits the largest surface area and porosity, whereas the zeolite ZS shows the smallest values of S_{sp} and V_{pore}. A high proportion of micropores is an important criterion for the effective use of a material as an adsorbent.

All three sorbents – activated carbon AC, silica gel SG, and zeolite ZS – are characterized by predominantly microporous structures. The activated carbon AC possesses the highest fraction of micropores, while the silica gel SG has the lowest.

Excess gas adsorption measurements were carried out at three different temperatures: 0, 22, and 50 °C. The adsorbates selected for the study were H_2 and its most common impurities – CO_2, CO, N_2 and CH_4. The excess adsorption isotherms of these gases on the sorbents at room temperature (22 °C) are shown in Fig. 2.

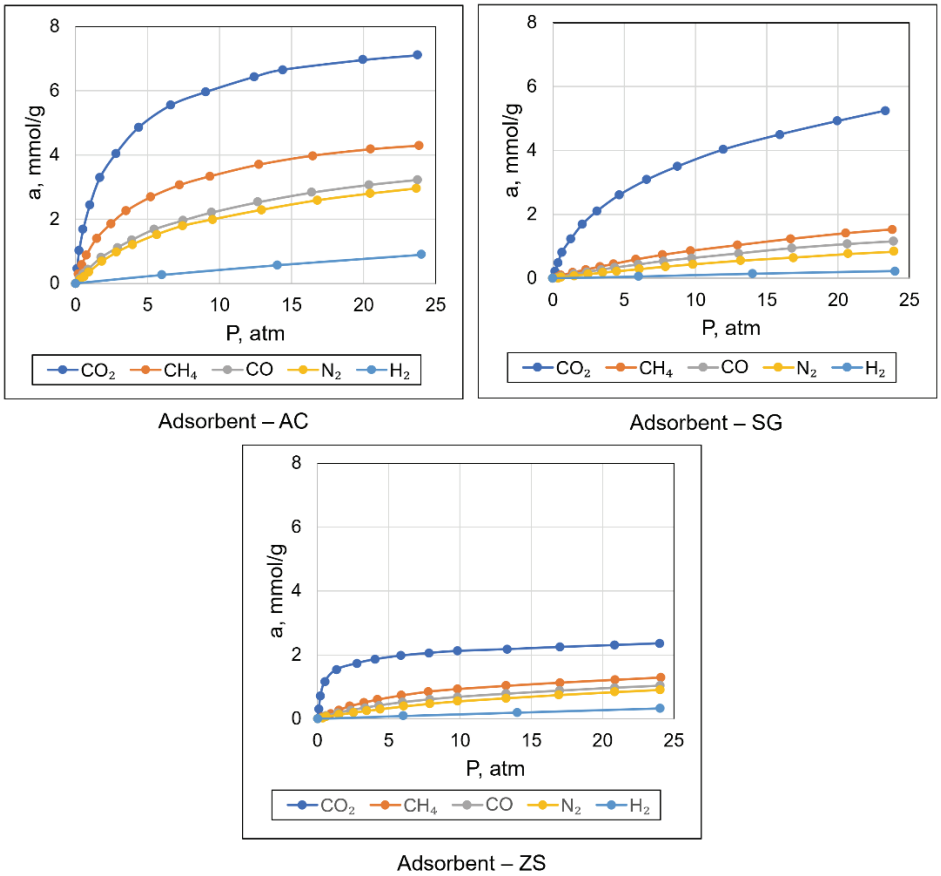

Fig. 2. Isotherms of excess gas adsorption on adsorbents at 22 °C

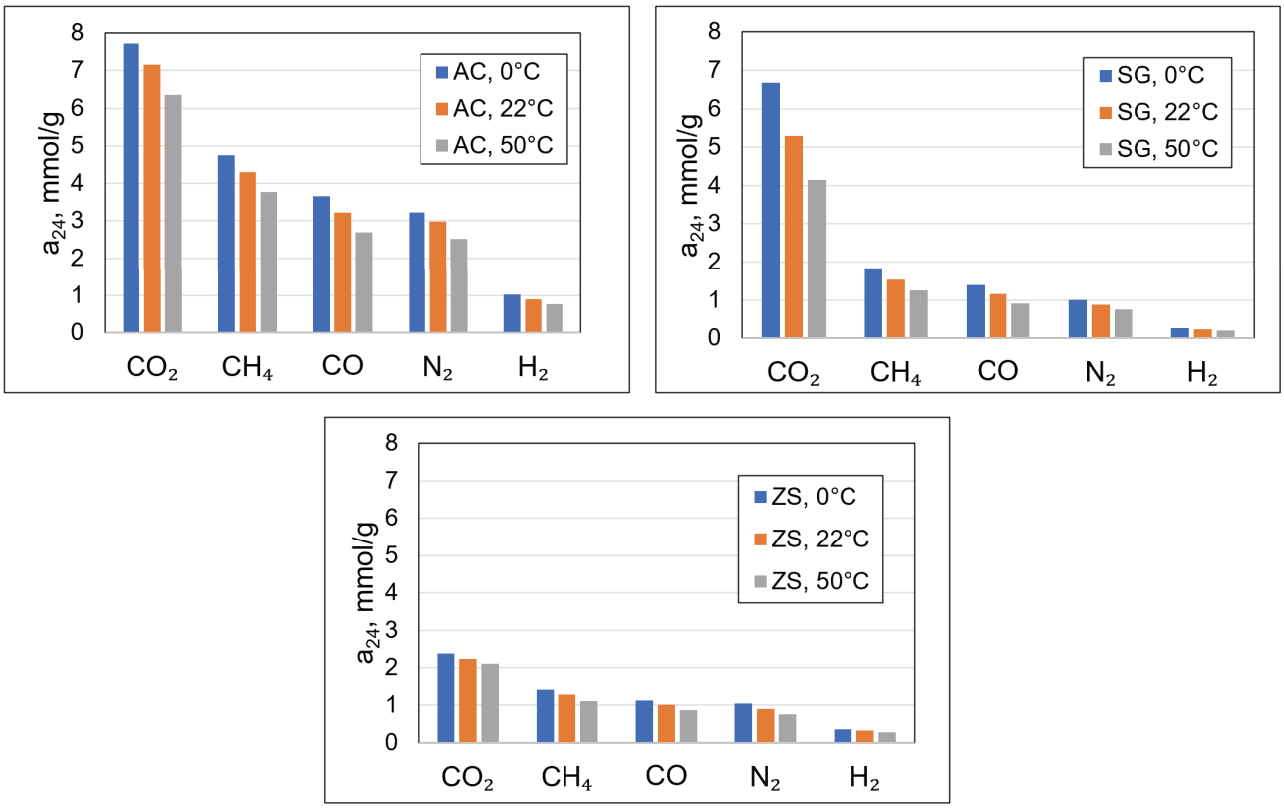

Fig. 3. Values of excess gas adsorption a_{24} at pressure P = 24 atm

For each of the three sorbents, the adsorption isotherms of methane (CH_4), carbon dioxide (CO_2), nitrogen (N_2), and carbon monoxide (CO) correspond to Type I isotherms according to the Brunauer classification [21]. The linear region of these isotherms lies within the pressure range up to 1–2 atm. The hydrogen adsorption isotherms on all sorbents are nearly linear and are well described by Henry's law.

For each gas adsorbent pair, the values of excess adsorption at the maximum pressure of 24 atm were determined and are presented in Fig. 3 on the same scale. The a_{24} values for a given gas/adsorbent pair decrease with increasing temperature, indicating the exothermic nature of the adsorption process.

The adsorption capacities of the gases for each adsorbent decrease in the following order: $CO_2 >> CH_4 > CO > N_2 >> H_2$, which is consistent with literature data for activated carbons [1] and silica gels [22]. For strongly polar zeolites, however, the adsorption sequence commonly reported in the literature is $CO_2 >> CO > CH_4 > N_2 >> H_2$ [1]. The deviation observed for the zeolite ZS may be attributed to a low number of adsorption sites for the polar CO and the highly polarizable CO_2 molecules with large quadrupole moments.

The calculated isosteric heats of adsorption in the temperature range 0 to 50 °C for CH_4, CO_2, CO, N_2, and H_2 are presented in Table 2.

Table 2. Values of isosteric heats of adsorption Q_{isost} for the studied gases

Gas	Adsorbent	Q_{isost}, kJ·mol^{-1}
CH_4	AC	15.5–17.5
	SG	15.3–16.9
	ZS	14.2–17.2
CO_2	AC	20.2–23.2
	SG	18.3–20.4
	ZS	13.5–25.5
N_2	AC	10.9–13.7
	SG	7.1–11.9
	ZS	9.0–12.6
CO	AC	13.8–16.1
	SG	11.3–15.7
	ZS	10.2–15.2
H_2	AC	4.1–6.3
	SG	3.8–5.2
	ZS	3.8–5.8

Based on the obtained adsorption isotherms for each impurity gas (CH_4, CO_2, N_2, and CO), the ideal selectivity coefficients relative to hydrogen were calculated as follows:

$$S_{\text{id}}(\text{X/H}_2) = \frac{a(\text{X})_{P,T}}{a(\text{H}_2)_{P,T}}, \quad (1)$$

where $a(\text{X})_{P,T}$ and $a(\text{H}_2)_{P,T}$ are the excess adsorptions of gas X and hydrogen H_2 on a given adsorbent at temperature *T* and pressure *P*.

The values of the ideal selectivity coefficients for each gas on activated carbon AC correlate well with literature data for BPL carbon. However, for zeolite ZS, the selectivities for CH_4/H_2 and N_2/H_2 pairs were found to be four times lower than those for commercial zeolite 5A; for CO/H_2, almost 16 times lower; and for CO_2/H_2, about two orders of magnitude lower than reported values. This reduction is attributed to a limited number of available adsorption sites capable of binding impurity gases on the adsorbent surface [1]. It is possible that the studied sorbents require more rigorous activation conditions than those recommended by the manufacturer and used in this work.

For the ideal selectivity coefficients $S_{\text{id}}(\text{X/H}_2)$, a decrease with increasing pressure *P* was observed, indicating higher gas separation efficiency at lower pressures. This behavior is due to the different shapes of the excess adsorption isotherms for impurity gases (Type I, according to Brunauer's classification) and for hydrogen (linear isotherm).

At low pressures, the ideal selectivity relative to hydrogen increases with decreasing temperature**.** This is associated with the higher heat of adsorption of impurity gases compared to hydrogen, leading to a greater increase in excess adsorption of the impurity gas under identical pressure conditions.

The ideal selectivity coefficients $S_{\text{id}}(\text{X/H}_2)$ account only for gas adsorption at equal partial pressures on pure adsorbents. Therefore, to model gas behavior in real multicomponent mixtures**,** other approaches must be applied–such as calculations using the IAST.

The IAST allows for the calculation of the excess adsorption of each gas component in a mixture based on their partial pressures in the gas phase and the adsorption isotherms of the pure gases.

The IAST selectivity coefficient for gas separation was calculated using the following equation, which accounts for the gas composition in the mixture:

$$S_{\text{IAST}}(\text{X/H}_2) = \frac{a_{\text{IAST}}(\text{X})\,\varphi(\text{H}_2)}{a_{\text{IAST}}(\text{H}_2)\,\varphi(\text{X})}, \quad (2)$$

where $\varphi(\text{X})$ and $\varphi(\text{H}_2)$ are the volume fractions of gas X and hydrogen in the gas mixture being separated, and $a_{\text{IAST}}(\text{X})$ and $a_{\text{IAST}}(\text{H}_2)$ are the real adsorption values obtained from the IAST model calculations.

The active adsorption sites on the surface are initially occupied by the most strongly adsorbed component (CO_2), followed by gases in the order $CH_4 > CO > H_2$. The competition for adsorption sites is also influenced by the composition of the equilibrium gas mixture above the adsorbent.

At present, the key method for hydrogen production is its purification using adsorption-based techniques from the products of natural gas steam reforming. The gas mixture (mixture 1) obtained after cooling of the reaction stream has the following composition: 70–80 % H_2, 15–25 % CO_2, 3–6 % CH_4, 1–3 % CO, and small amounts of N_2 impurities.

To perform a preliminary selection of the adsorbent and determine the optimal conditions for hydrogen purification from impurities in *gas mixture 1*, IAST modeling was applied to a *model gas mixture* with the following composition: 73.5 % H_2, 20 % CO_2, 4.5 % CH_4, and 2.0 % CO. This composition corresponds to the average impurity content of CO_2, CH_4, and CO in the real gas *mixture 1* subjected to purification.

Below is a comparison of the ideal selectivity coefficients with the IAST separation selectivity coefficient**s** in the Henry's law region (Table 3) and at a pressure of 20 atm (Table 4).

For each sorbent in the Henry's law region ($P < 1$ atm), the selectivity coefficient according to IAST for the CO_2/H_2 pair, $S_{\text{IAST}}(CO_2/H_2)$, is higher than the ideal selectivity $S_{\text{id}}(CO_2/H_2)$ at 0, 22, and 50°C. This is due to the preferential adsorption of carbon dioxide, which has the greatest affinity for the sorbent. The largest difference between $S_{\text{IAST}}(CO_2/H_2)$ and $S_{\text{id}}(CO_2/H_2)$ is observed for zeolite ZS, which effectively adsorbs carbon dioxide in the low-pressure region. This is reflected in the shape of the corresponding excess adsorption isotherm.

For CH_4 and CO, the values of $S_{\text{IAST}}(\text{X/H}_2)$ are comparable to $S_{\text{id}}(\text{X/H}_2)$. Recalculation using the IAST model has almost no effect on selectivity, since the adsorption values of CO, CH_4, and H_2 decrease to a similar extent due to competition with the more strongly adsorbed CO_2.

Table 3. Comparison of ideal selectivity coefficients S_{id} and IAST selectivity coefficients S_{IAST} in the Henry's law region

Adsorbent	Gas	0 °C		22 °C		50 °C	
		$S_{id}(X/H_2)$	$S_{IAST}(X/H_2)$	$S_{id}(X/H_2)$	$S_{IAST}(X/H_2)$	$S_{id}(X/H_2)$	$S_{IAST}(X/H_2)$
AC	CO_2	90.0	113.4	72.8	83.2	54.8	62.5
	CH_4	38.3	36.9	32.2	30.5	32.2	21.4
	CO	20.0	17.0	15.1	12.9	11.9	9.4
SG	CO_2	104.3	157.2	99.9	125.7	93.2	103.0
	CH_4	12.8	14.6	12.3	13.5	11.8	12.6
	CO	10.7	12.4	9.3	10.1	8.0	8.8
ZS	CO_2	80.1	216.1	75.1	188.7	69.9	127.3
	CH_4	15.3	20.2	12.4	13.9	9.5	9.7
	CO	8.4	10.1	8.0	9.2	7.7	8.0

Table 4. Comparison of ideal selectivity coefficients S_{id} and selectivity coefficients according to IAST S_{IAST} at 20 atm

Adsorbent	Gas	0 °C		22 °C		50 °C	
		$S_{id}(X/H_2)$	$S_{IAST}(X/H_2)$	$S_{id}(X/H_2)$	$S_{IAST}(X/H_2)$	$S_{id}(X/H_2)$	$S_{IAST}(X/H_2)$
AC	CO_2	8.9	57.3	8.7	46.8	8.5	32.9
	CH_4	5.4	11.8	5.3	11.4	5.1	11.3
	CO	4.0	5.0	3.9	4.8	3.8	4.7
SG	CO_2	28.9	105.4	25.3	84.2	22.2	61.8
	CH_4	7.7	7.6	7.1	7.4	6.5	7.1
	CO	5.9	4.6	5.4	4.4	4.7	4.2
ZS	CO_2	8.3	70.7	7.9	65.8	7.6	54.0
	CH_4	4.4	4.6	4.3	4.4	4.2	4.3
	CO	3.5	4.2	3.4	3.6	3.2	3.1

For the gas separation selectivity coefficients calculated by IAST, $S_{IAST}(X/H_2)$ in the Henry's law region – as across the entire pressure range – a decrease in selectivity is observed with increasing temperature. Therefore, lowering the process temperature can enhance the efficiency of gas mixture separation.

As with the ideal selectivity coefficients $S_{id}(X/H_2)$, the IAST selectivity coefficients $S_{IAST}(X/H_2)$ also decrease with increasing total mixture pressure (Table 4), indicating that gas separation is more effective in the low-pressure region. However, separation at low pressures is practically impossible in the case of pressure swing adsorption (PSA) processes, since desorption typically occurs in the low-pressure range, while adsorption takes place at higher pressures – from 8 to 28 atm.

Depending on the total gas mixture pressure and experimental temperature, the most effective sorbent for CO_2 removal can be either zeolite ZS ($P < 12$ atm at 22 °C) or silica gel SG ($P > 12$ atm at 22 °C). Activated carbon AC can be used for the most effective removal of CO and CH_4 impurities from gas mixtures.

Thus, from the standpoint of real gas separation selectivity calculated using IAST theory, hydrogen purification from impurities is most effective at the lowest possible temperature and under low-pressure conditions. Under these conditions, zeolite ZS is the

most efficient for removing CO_2 impurities, while activated carbon AC is most effective for removing CH_4 and CO. For gas mixture separation at higher pressures (above 12 atm, which is closer to real operating conditions), silica gel SG is preferable for CO_2 removal, and activated carbon AC remains the best option for CH_4 and CO removal.

4. Conclusion

The surface morphology and structure of commercial adsorbents – activated carbon AC, silica gel SG, and zeolite ZS – have been studied. All of these materials belong to the class of microporous materials, with a micropore fraction ranging from 79 to 92 %. The highest specific surface area ($S_{sp} = 994$ $m^2 \cdot g^{-1}$) and pore volume ($V_{pore} = 0.44$ $cm^3 \cdot g^{-1}$) are observed for AC, while the lowest values are found for ZS ($S_{sp} = 408$ $m^2 \cdot g^{-1}$, $V_{pore} = 0.25$ $cm^3 \cdot g^{-1}$). Excess adsorption isotherms for hydrogen and impurity gases (CO_2, CH_4, CO, N_2) were measured at temperatures from 0 to 50 °C and pressures up to 25 atm. It was found that the highest adsorption occurs on AC, and the adsorption order of gases follows the trend: $CO_2 >> CH_4 > CO > N_2 >> H_2$. The highest isosteric heats of adsorption for most gases were observed for activated carbon AC, which possesses the largest S_{sp} and V_{pore} values. Calculations of adsorption selectivity coefficients for impurity gas/hydrogen pairs using the IAST model show that $S_{IAST}(CO_2/H_2)$ increases by a factor of 1.5–3 compared to S_{id} (CO_2/H_2), while for other gases, the coefficients are comparable.

5. Funding

The study was carried out within the framework of state assignment No. 122012400186-9.

6. Acknowledgements

The authors thank JSC Grasys for providing the adsorbent samples.

7. Conflict of interest

The authors declare no conflict of interest.

References

1. Sircar S, Golden TC. Purification of hydrogen by pressure swing adsorption. *Separation Science and Technology*. 2000;35(5):667-687. DOI:10.1081/SS-100100183

2. Kozlov S, Fateyev V. *Hydrogen energy: current state, problems, prospects*. Moscow: Gazprom VNIIGAZ; 2009. 518 p. (In Russ.)

3. Du Z, Liu C, Zhai J, Guo X, et al. A review of hydrogen purification technologies for fuel cell vehicles. *Catalysts*. 2021;11(3):393. DOI:10.3390/catal11030393

4. Zhang R, Shen Y, Tang Z, Li W, et al. A review of numerical research on the pressure swing adsorption process. *Processes*. 2022;10(5):812. DOI:10.3390/pr10050812

5. Grande CA. Advances in pressure swing adsorption for gas separation. *ISRN Chemical Engineering*. 2012;2012:1-13. DOI:10.5402/2012/982934

6. Lopes FVS, Grande CA, Rodrigues AE. Fast-cycling VPSA for hydrogen purification. *Fuel*. 2012;93:510-523. DOI:10.1016/j.fuel.2011.07.005

7. Shah G, Ahmad E, Pant KK, Vijay VK. Comprehending the contemporary state of art in biogas enrichment and CO_2 capture technologies via swing adsorption. *International Journal of Hydrogen Energy*. 2021;46(9):6588-6612. DOI:10.1016/j.ijhydene.2020.11.116

8. Sircar S, Golden TC, Rao MB. Activated carbon for gas separation and storage. *Carbon*. 1996;34(1):1-12. DOI:10.1016/0008-6223(95)00128-X

9. Cundy CS, Cox PA. The hydrothermal synthesis of zeolites: history and development from the earliest days to the present time. *Chemical Reviews*. 2003;103(3):663-702. DOI:10.1021/cr020060i

10. Sadighi S., Soleymani R. Synthesis of 5A molecular sieve for hydrogen purification in pressure swing adsorbers. *2nd Iran National Zeolite Conference (2INZC)*. 2015. p. 27-8.

11. Orsikowsky-Sanchez A, Franke C, Sachse A, Ferrage E, et al. Gas porosimetry by gas adsorption as an efficient tool for the assessment of the shaping effect in commercial zeolites. *Nanomaterials*. 2021;11(5):1205. DOI:10.3390/nano11051205

12. Yan KL, Wang Q. Adsorption characteristics of the silica gels as adsorbent for gasoline vapors removal. *IOP Conference Series: Earth and Environmental Science*. 2018;153(2):022010. DOI:10.1088/1755-1315/153/2/022010

13. *BASF: Sorbead®*. Available from: https://chemical-catalysts-and-adsorbents.basf.com/global/en/adsorbents/sorbead-for-ccs [Accessed 09 Jule 2025]

14. Myers AL, Prausnitz JM. Thermodynamics of mixed-gas adsorption. *AIChE Journal*. 1965;11(1):121-127. DOI:10.1002/aic.690110125

15. Frenkel D, Smit B. *Understanding molecular simulation: from algorithms to applications*. San Diego: Academic Press; 2002. 638 p. (Computational science series).

16. Simon CM, Smit B, Haranczyk M. PyIAST: ideal adsorbed solution theory (IAST) python package. *Computer Physics Communications*. 2016;200:364-380. DOI:10.1016/j.cpc.2015.11.016

17. *National institute of standards and technology*. Thermophysical properties of fluid systems n.d. Available from: https://webbook.nist.gov/chemistry/fluid/ [Accessed 17 May 2025].

18. Keppetipola NM, Dissanayake M, Dissanayake P, Karunarathne B, et al. Graphite-type activated carbon from coconut shell: a natural source for eco-friendly non-volatile storage devices. *RSC Advances*. 2021;11(5):2854-2865. DOI:10.1039/D0RA09182K

19. Chen L, Wang YW, He MY, Chen Q, et al. Facile synthesis of 5A zeolite from attapulgite clay for adsorption of n-paraffins. *Adsorption*. 2016;22(3):309-314. DOI:10.1007/s10450-016-9776-y

20. Keller J, Staudt R. *Gas adsorption equilibria. Experimental Methods and Adsorptive Isotherms*. Boston: Springer Science + Business Media, Inc; 2005. 422 p.

21. Karnaukhov A. *Adsorption. The texture of dispersed and porous materials*. Novosibirsk: Nauka Publ. Siberian Enterprise of the Russian Academy of Sciences; 1999. 469 p. (In Russ.)

22. Jung J, Do H, Chung K, Cho M, et al. Adsorption equilibria and kinetics of CO_2, CH_4, CO, N_2, O_2, and H_2 on silica-based adsorbents for H_2 enhancement processes from steel off-gas for the direct reduced iron process. *Chemical Engineering Journal*. 2024;479:147678. DOI:10.1016/j.cej.2023.147678

Information about the authors / Информация об авторах

Nikita S. Krysanov, PhD Student, Lomonosov Moscow State University (MSU), Moscow, Russian Federation; ORCID 0009-0003-4811-7021; e-mail: n.krysanov@mail.ru

Elena A. Berdonosova, Cand. Sc. (Chem.), Senior Researcher, MSU, Moscow, Russian Federation; ORCID 0000-0002-4580-9749; e-mail: ellenganich@highp.chem.msu.ru

Semen N. Klyamkin, D. Sc. (Chem.), Professor, MSU, Moscow, Russian Federation; ORCID 0000-0001-6009-1045; e-mail: klyamkin@highp.chem.msu.ru

Крысанов Никита Сергеевич, аспирант, Московский государственный университет имени М. В. Ломоносова (МГУ), Москва, Российская Федерация; ORCID 0009-0003-4811-7021; e-mail: n.krysanov@mail.ru

Бердоносова Елена Александровна, кандидат химических наук, старший научный сотрудник, МГУ, Москва, Российская Федерация; ORCID 0000-0002-4580-9749; e-mail: ellenganich@highp.chem.msu.ru

Клямкин Семен Нисонович, доктор химических наук, профессор, МГУ, Москва, Российская Федерация; ORCID 0000-0001-6009-1045; e-mail: klyamkin@highp.chem.msu.ru

Received 16 July 2025; Revised 08 September 2025; Accepted 11 September 2025